

Submicrojoule femtosecond erbium-doped fibre laser for the generation of dispersive waves at submicron wavelengths

L.V. Kotov, M.Yu. Koptev, E.A. Anashkina, S.V. Muravyev, A.V. Andrianov, M.M. Bubnov, A.D. Ignat'ev, D.S. Lipatov, A.N. Gur'yanov, M.E. Likhachev, A.V. Kim

Abstract. We have demonstrated a femtosecond erbium-doped fibre laser system built in the master oscillator/power amplifier (MOPA) approach. The final amplifier stage utilises a specially designed large mode area active fibre cladding-pumped by multi-mode laser diodes. The system is capable of generating submicrojoule pulses at a wavelength near 1.6 μm . We have obtained 530-fs pulses with an energy of 400 nJ. The output of the system can be converted to wavelengths shorter than 1 μm through the generation of dispersive waves in passive nonlinear fibre. We have obtained ultra-short 7-nJ pulses with a spectral width of ~ 100 nm and a centre wavelength of 0.9 μm , which can be used as a seed signal in parametric amplifiers in designing petawatt laser systems.

Keywords: high peak power fibre laser systems, erbium-doped fibre amplifiers, large mode area fibres, ultra-short pulses, dispersive waves.

1. Introduction

Advances in the development of near-IR fibre laser systems for the generation of high peak power ultra-short pulses are

driven largely by the necessity of addressing practical issues in two-photon spectroscopy, biomedicine, precision materials processing, etc. At present, wide use is made of laser systems that employ erbium-doped active fibres and mature optical fibre communication technologies [1]. Inferior in energy performance to solid-state systems, fibre lasers and nonlinear optical fibre devices offer the advantages of high pump conversion efficiency (due to the particular guiding geometry), efficient heat dissipation, high quality of the spatial laser beam profile, low cost, compactness and requiring no alignment during operation.

The most widespread laser configurations take advantage of the master oscillator/power amplifier (MOPA) approach [1]. Since the energy of the forming signal is often limited by the nonlinear properties of the active fibres in the final stage of the amplifier, chirped-pulse amplification (CPA) is utilised to reach high pulse energies, and external dispersive compressors that include bulk elements – prisms, gratings or their combinations – are used for frequency modulation compensation [1, 2]. One common approach for reducing nonlinear effects is to employ large mode area (LMA) fibres, which allows pulses with high energies and high peak powers to be obtained [3–5]. Note that, in the case of cladding-pumped erbium-doped fibres, increasing the core diameter is necessary not only for reducing nonlinear effects but also for creating an acceptable inversion [6].

In this work, we examine two high peak power erbium-doped fibre MOPA laser configurations, which employ the same master oscillator and a specially designed LMA active fibre in the final amplifier stage. The system is capable of lasing in two modes, generating submicrojoule ~ 500 -fs pulses in CPA mode (with the use of a grating compressor) and ~ 10 -nJ ~ 100 -fs pulses in an all-fibre configuration, with no external compressor. In addition to other potential applications, the system can be effectively used to produce ultra-short pulses at submicron wavelengths through the generation of dispersive waves, which have been the subject of extensive studies (see e.g. Refs [7–12]).

A fibre source of broadband femtosecond optical pulses with a centre wavelength near 0.9 μm can be used as a master oscillator in optical parametric chirped-pulse amplifiers (OPCPAs) based on large-aperture DKDP crystals [13]. To date, a peak power of 0.56 PW has been reached in such amplifiers [14]. In this work, a signal with a centre wavelength of 0.9 μm and a bandwidth of 100 nm has been experimentally demonstrated, which may have important practical implications for the development of OPCPAs with peak powers of several petawatts.

L.V. Kotov Fiber Optics Research Center, Russian Academy of Sciences, ul. Vavilova 38, 119333 Moscow, Russia; Moscow Institute of Physics and Technology (State University), Institutskii per. 9, 141700 Dolgoprudnyi, Moscow region, Russia;

M.Yu. Koptev, S.V. Muravyev, A.V. Andrianov Institute of Applied Physics, Russian Academy of Sciences, ul. Ul'yanova 46, 603950 Nizhnii Novgorod, Russia; e-mail: max-koptev@ya.ru, alex.v.andrianov@gmail.com;

E.A. Anashkina, A.V. Kim Institute of Applied Physics, Russian Academy of Sciences, ul. Ul'yanova 46, 603950 Nizhnii Novgorod, Russia; N.I. Lobachevsky Nizhnii Novgorod State University, prosp. Gagarina 23, 603950 Nizhnii Novgorod, Russia; e-mail: elena.anashkina@gmail.com, kim@ufp.appl.sci-nnov.ru;

M.M. Bubnov, M.E. Likhachev Fiber Optics Research Center, Russian Academy of Sciences, ul. Vavilova 38, 119333 Moscow, Russia; e-mail: likhachev@fo.gpi.ru, bubnov@fo.gpi.ru;

A.D. Ignat'ev FORC-Photonics Group, ul. Vavilova 38, 119333 Moscow, Russia;

D.S. Lipatov N.I. Lobachevsky Nizhnii Novgorod State University, prosp. Gagarina 23, 603950 Nizhnii Novgorod, Russia; G.G. Devyatikh Institute of Chemistry of High-Purity Substances, Russian Academy of Sciences, ul. Tropinina 49, 603950 Nizhnii Novgorod, Russia; e-mail: lipatovds@mail.ru;

A.N. Gur'yanov G.G. Devyatikh Institute of Chemistry of High-Purity Substances, Russian Academy of Sciences, ul. Tropinina 49, 603950 Nizhnii Novgorod, Russia

Received 3 March 2014; revision received 12 March 2014

Kvantovaya Elektronika 44 (5) 458–464 (2014)

Translated by O.M. Tsarev

2. Erbium-doped LMA fibre design optimisation

The concept of building a high-power MOPA laser system relies on the use of a fibre seed laser, a three-stage chirped-pulse amplifier having an LMA fibre final stage and a dispersive grating compressor.

A factor that plays a key role in limiting the maximum pulse energy is the threshold for nonlinear effects in the final amplifier stage. For this reason, it is the optimisation of the final amplifier stage that has been the subject of considerable effort in this investigation. In a recent study [15], a novel design was proposed for a double-clad erbium-doped LMA fibre having a 35- μm -diameter core and codoped with aluminium and fluorine. The fibre composition made it possible, on the one hand, to sufficiently suppress erbium ion clustering (owing to the relatively high aluminium oxide concentration) [16] and, on the other, to reduce the core-cladding refractive index difference to $\Delta n \approx 0.0012$ (due to fluorine doping), which ensured single-mode operation of the fibre even at relatively large bend radii.

The dashed line in Fig. 1 shows a calculated pump (980 nm) to signal (1585 nm) conversion efficiency as a function of erbium ion concentration for an aluminosilicate fibre amplifier having the design in question. It is seen that efficiencies up to 40% are possible, but only at relatively low erbium concentrations, which makes it necessary to use a 40 to 50 m length of active fibre [15]. Even though this length is not critical for cw lasers and amplifiers, it is unacceptable for short-pulse amplification because of the low threshold for nonlinear effects in this case. The length of the active fibre can be reduced by increasing the erbium concentration in the core, but this is accompanied by a substantial drop in efficiency (Fig. 1), which is caused by stronger erbium ion clustering [15]. As shown by Likhachev et al. [17], the use of a phosphoaluminosilicate glass host in the fibre core allows the degree of clustering to be reduced. Note also that, when the aluminium and phosphorus concentrations differ little, fibres with arbitrary small Δn can be produced, which allows one to fabricate large core diameter single-mode fibres. The solid line in Fig. 1 represents calculation results for phosphoaluminosilicate fibres with core and cladding diameters of 35 and 125 μm , respectively. It is seen that, even though the maximum obtainable efficiency changes little, the efficiency decreases considerably more gradually with increasing doping level than it

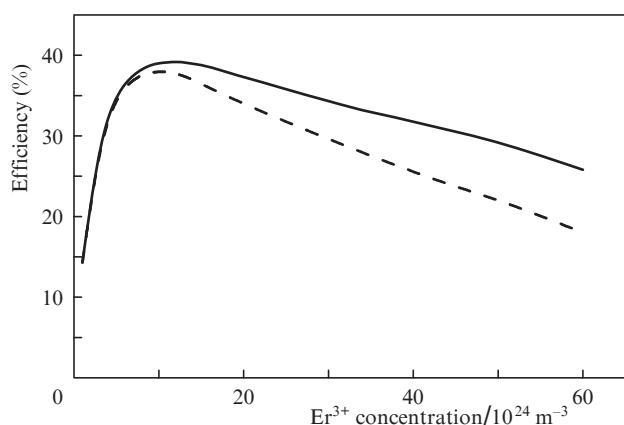


Figure 1. Calculated pump (980 nm) to signal (1585 nm) conversion efficiency for erbium-doped LMA aluminosilicate (dashed line) and phosphoaluminosilicate (solid line) fibres.

does in the case of the aluminosilicate glass core. Thus, erbium-doped fibres with an $\text{Al}_2\text{O}_3\text{-P}_2\text{O}_5\text{-SiO}_2$ core are better suited for producing high nonlinear threshold amplifiers than are standard aluminosilicate fibres.

3. Characteristics of the fibre and amplifier

An erbium-doped fibre preform was fabricated by the MCVD process. Its core contained ~ 7 mol% Al_2O_3 , ~ 8 mol% P_2O_5 and ~ 0.1 mol% Er_2O_3 . The preform was then drawn into fibre in polymer coating, which ensured a numerical aperture of ~ 0.46 for pump radiation. To improve pump absorption, the cladding had a square cross section with a side length of 115 μm . Its area is roughly equal to the cross-sectional area of a 125- μm -diameter round fibre, which allows the active fibre to be fusion-spliced to standard pump/signal combiners with negligible pump loss. The small-signal pump absorption was 3 dB m^{-1} at a wavelength of 980 nm. The measured refractive index profile and fundamental mode field distribution at 1550 nm are presented in Fig. 2. The mode field diameter was determined to be 24.7 μm and the group velocity dispersion at a wavelength of 1.56 μm was estimated at 27 ps nm^{-1} km^{-1} .

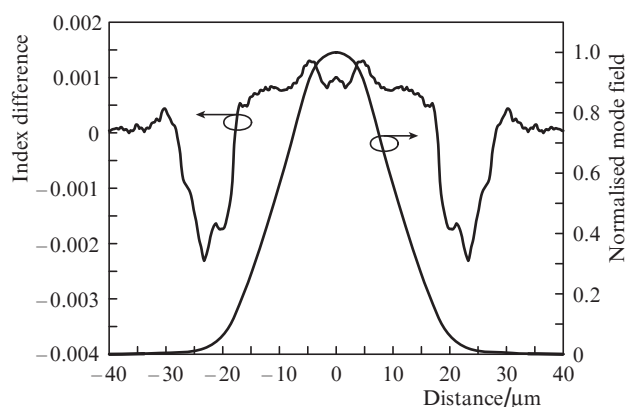


Figure 2. Refractive index difference (experiment) and fundamental mode field distribution (calculation) for erbium-doped LMA fibre.

To optimise the fibre length in the amplifier, we measured the pump-to-signal conversion efficiency as a function of signal wavelength at active fibre lengths of 6 and 3.5 m using cladding pumping in a copropagating pump scheme. As seed sources, we used fibre lasers with an emission bandwidth under 1 nm and an output power of ~ 100 mW, which corresponded to power amplification. The results obtained are presented in Fig. 3, where one can see that, as the fibre length decreases from 6 to 3.5 m, the wavelength corresponding to the maximum narrow-band signal amplification efficiency shifts from 1575 to 1560 nm. It is worth noting that the overall decrease in efficiency is caused by the increase in the percentage of unabsorbed pump light with decreasing fibre length. Moreover, in the case of ultra-short pulse amplification, the emission spectrum is rather broad and may be distorted because the gain coefficient is wavelength-dependent.

To examine the feasibility of using the proposed amplifier as a final stage of a CPA scheme, gain spectra were also investigated. As a signal, we used the output of a cw superluminescent erbium-doped fibre source operating in the range 1520–1600 nm. Figure 4 shows measured gain spectra of a

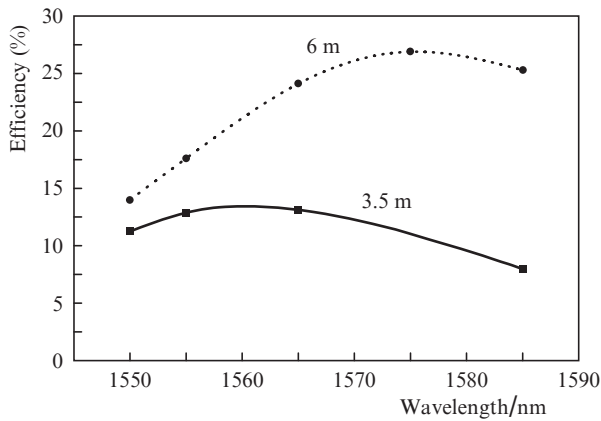


Figure 3. Pump-to-signal conversion efficiency as a function of wavelength for 3.5- and 6-m lengths of erbium-doped LMA fibre.

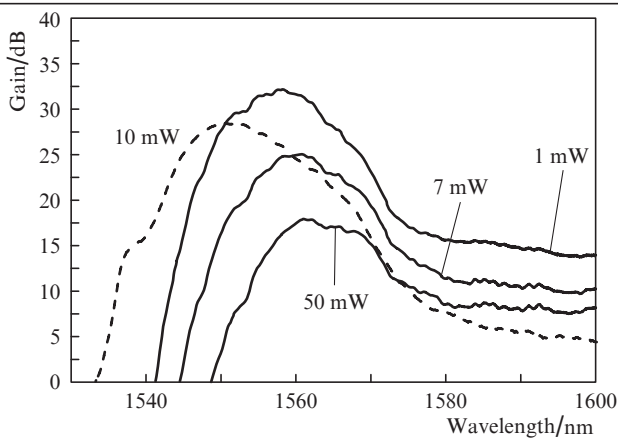


Figure 4. Gain spectra at the output of the erbium-doped LMA fibres 3.5 (dashed line) and 6 m (solid lines) in length at different input signal powers.

6-m length of the erbium-doped fibre at input signal powers of 1, 7 and 50 mW and an output power of ~ 1 W and the gain

spectrum of a 3.5-m length of the fibre at a 10-mW input power and 2-W output. It is seen that reducing the input signal power increases the gain coefficient at the short-wavelength edge of the spectrum because of the increase in population inversion. At the same time, it has been shown previously [15] that, when a narrow-band signal is amplified, an increase in population inversion with decreasing wavelength increases the adverse effect of clustering and, as a consequence, reduces the efficiency of double-clad erbium-doped fibres. This accounts for the fact that the peak broadband gain wavelength (1563 nm) (Fig. 4) differs from the wavelength (1575 nm) corresponding to the highest efficiency (Fig. 3). It also follows from Fig. 4 that the peak gain wavelength can be reduced substantially by reducing the active fibre length. At both erbium-doped fibre lengths, the 3-dB gain bandwidth was determined to be ~ 15 nm. Despite its lower efficiency, the 3.5-m erbium-doped fibre amplifier had a higher threshold for nonlinear effects, so it was this amplifier which was used to construct a CPA scheme.

4. Development of a femtosecond submicrojoule laser system (CPA scheme)

A schematic of the experimental setup is shown in Fig. 5. Basic to this configuration is a previously developed femtosecond ring-cavity erbium-doped fibre laser diode-pumped at 975 nm. The laser is passively mode-locked using a nonlinear rotation of the polarisation ellipse of a femtosecond pulse due to the optical Kerr effect. The seed laser generates 230-fs, 1.56- μm pulses at a repetition rate of 50 MHz [10]. After it, the scheme contains a Faraday isolator and a fibre stretcher consisting of two series-connected germanosilicate fibre segments 40 and 55 m in length, with 1.56 μm group velocity dispersions of -54 and -37 ps nm^{-1} km^{-1} , respectively. The stretcher slightly broadens the spectrum due to the self-phase modulation in the initial portion of propagation. The chirped pulses are amplified in the first erbium-doped fibre preamplifier to 50 mW of average power, and then the pulse repetition rate is reduced to 1 MHz by an acousto-optic modulator

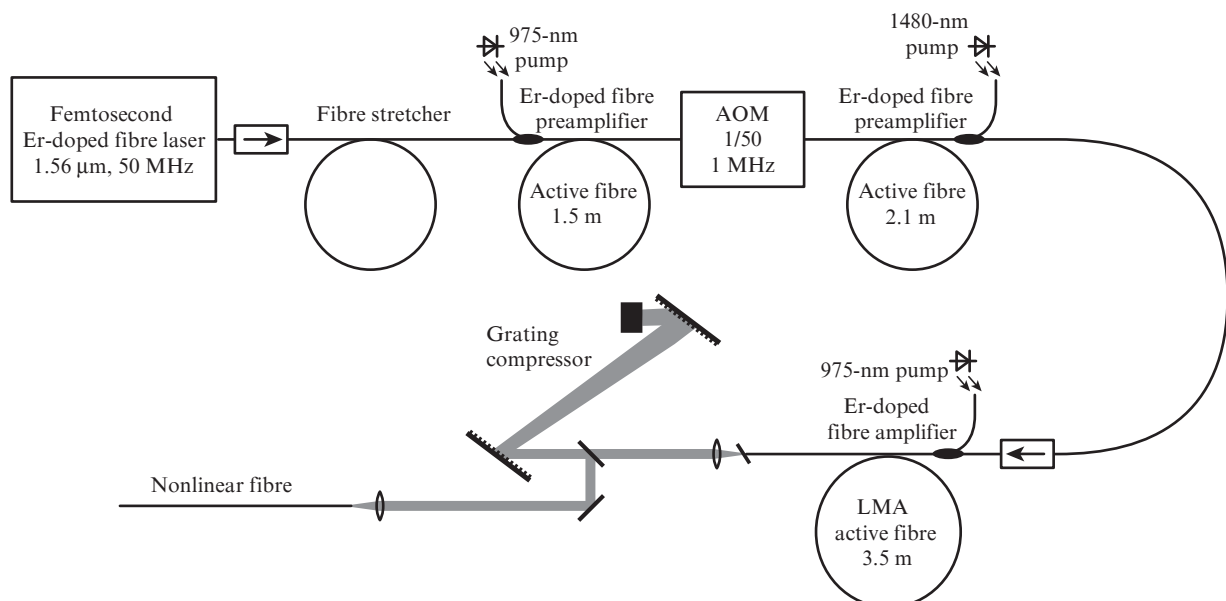


Figure 5. Schematic of the CPA setup.

(AOM) in order to reduce the required average pump power in the final amplifier stage, where submicrojoule pulses are formed. The decimated pulse sequence is amplified in the second preamplifier to an average power of 5 mW. Figure 6 shows the spectra of the signal after the stretcher and each preamplifier. The gain band of the active fibres is narrower

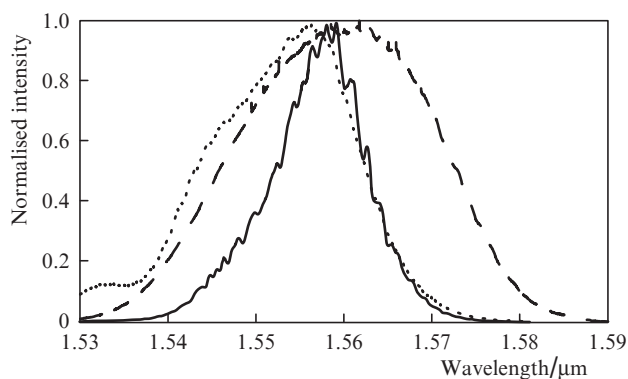


Figure 6. Spectra of the signal in CPA mode after the stretcher (dashed line), first preamplifier (dotted line) and second preamplifier (solid line).

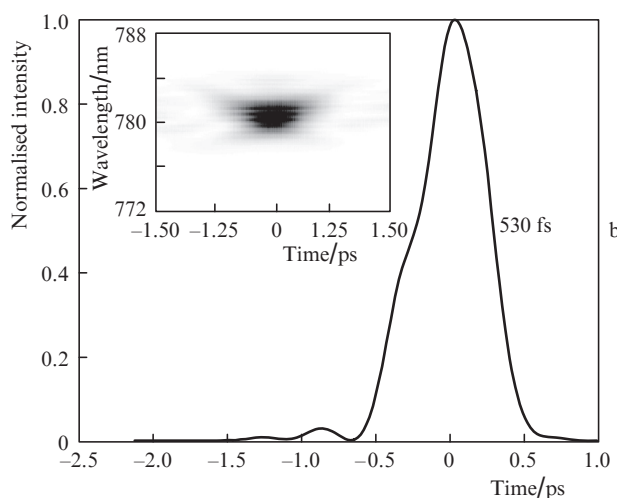
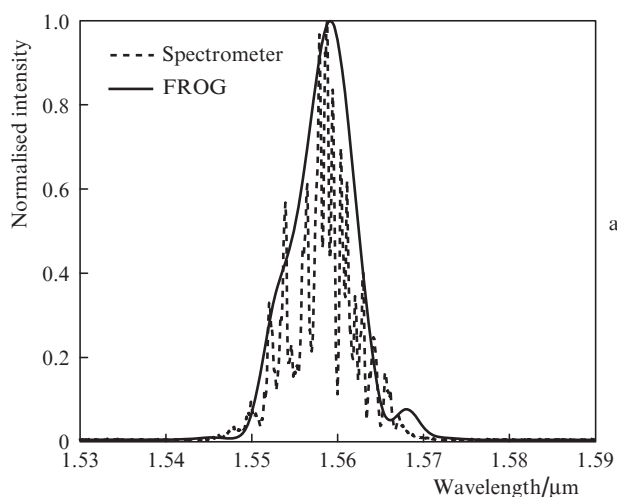


Figure 7. (a) Spectra of the signal after the dispersive compressor: measured with a spectrometer (dashed line) and FROG-retrieved (solid line); (b) FROG-retrieved temporal pulse profile.

than the spectrum of the input signal, so both amplifier stages reduce the width of the spectrum in CPA mode.

After the second preamplifier, the pulses pass through a Faraday isolator and arrive at the final stage, made from the specially designed erbium-doped LMA fibre. At the output of the 3.5-m-long fibre, we obtained a signal with an average power of 1 W, which corresponded to a pulse energy of $\sim 1 \mu\text{J}$ at an estimated pulse duration of ~ 50 ps. The output signal power was limited by the pump power. The frequency modulation of the amplified pulses was compensated using a dispersive compressor consisting of 600 lines mm^{-1} diffraction grating pair (Spectrogon). After the compressor, the pulse duration was 530 fs. Because of the low efficiency of the compressor in the 1.55- μm range, the maximum average power after compression was 400 mW, which corresponded to an energy of ~ 400 nJ. To diagnose the nature of the pulses, we used frequency-resolved optical gating (FROG) [18]. From an experimental set of spectra of the sum harmonic from two replicas of the pulses measured with different time delays relative to each other, we reconstructed the temporal and spatial pulse intensity and phase profiles using an iteration algorithm.

Figure 7 shows experimentally determined and FROG-retrieved spectra of the signal after the dispersive compressor and the temporal pulse intensity profile. The pulse time–bandwidth product is $\text{TBP} = 0.5$. An order of magnitude estimate of the pulse peak power as the pulse energy to duration ratio gives 750 kW.

5. Conversion of submicrojoule pulses in nonlinear silica fibre in an ultra-broad spectral range

The submicrojoule pulses obtained in the CPA mode were used in our experiments aimed at converting radiation in an ultra-broad spectral range, spanning more than an octave. After the dispersive compressor, the beam was launched into a 1.5-m segment of Flexcore 1060 nonlinear fibre using a lens (Fig. 5). The average output signal power was 100 mW. The spectrum in Fig. 8 clearly shows a peak at a centre wavelength of 0.9 μm , whose 3-dB width is 100 nm. The average signal power as measured with a Thorlabs S120C silicon photodiode, which detects light in the range 400–1100 nm, is 7.5 mW, which corresponds to a pulse energy of ~ 7 nJ at the centre wavelength 0.9 μm . In addition, the spectrum of the signal contains long-wavelength components. The width of the supercontinuum is 1400 nm (from 0.8 to 2.2 μm).

The most efficient mechanism of short-wavelength radiation formation is the generation of linear dispersive waves in

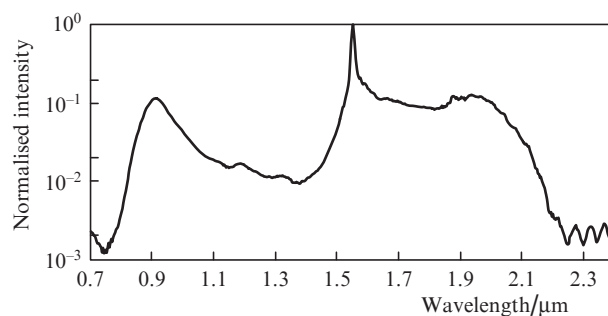


Figure 8. Spectrum of the signal at the nonlinear fibre output under pumping with the output of the system in CPA mode.

the normal dispersion region of optical fibre upon compression during the propagation of a high-order soliton in the anomalous dispersion region [7]. Note that fibre-optic converters rely on this mechanism to produce high-quality coherent radiation in an ultra-broad spectral range, inaccessible to lasers [9]. The experimental result of femtosecond pulse conversion from the 1.5- μm range to wavelengths between 0.8 and 1 μm is quite consistent with theoretical assessment of its feasibility [12]. Previous experimental studies also demonstrated the generation of dispersive wave packets at a wavelength near 1 μm at an initial 1.5- μm signal energy of ~ 2 nJ [10, 11]. In this study, the formation of shorter wavelength radiation was possible owing to the increase in signal energy by two orders of magnitude.

The long-wavelength wing of the spectrum is formed by sequentially produced solitons, whose centre wavelength gradually shifts during propagation along the fibre as a result of SRS [19].

Thus, the erbium-doped fibre laser configuration under consideration can be successfully used both to produce broadband radiation at a wavelength under 1 μm and generate supercontinuum spanning more than an octave.

6. Generation of 100-fs pulses of 100-kW peak power in an all-fibre configuration with no external compressor

We also examined the possibility of generating high peak power femtosecond pulses merely by optimising parameters of a normal dispersion stretcher, with no external compressor. In this case, the system is all-fibre, which makes it quite convenient for applications. Figure 9 shows a schematic of the experimental setup. After the Faraday isolator, the pulses were amplified in an erbium-doped fibre preamplifier to an average power of 150 mW, chirped in a 3.5-m length of fibre with a dispersion of -37 ps nm $^{-1}$ km $^{-1}$ at 1.56 μm and amplified in an erbium-doped LMA fibre, also 3.5 m in length, to an average power of ~ 700 mW. The pump-to-signal energy conversion efficiency was 10%.

While propagating along the anomalous dispersion amplifier, the signal was compressed as a result of chirp compensation. Moreover, compression at high peak powers may be caused as well by high-order soliton effects [19, 20]. At a large length of normal dispersion fibre, chirp compensation is incomplete, and the output pulse remains frequency-modulated. At small stretcher lengths, several scenarios are possible, as a result of which the pulse may be amplified as a whole or sequentially break up into two or more pulses [20]. We are interested here in single-pulse amplification mode.

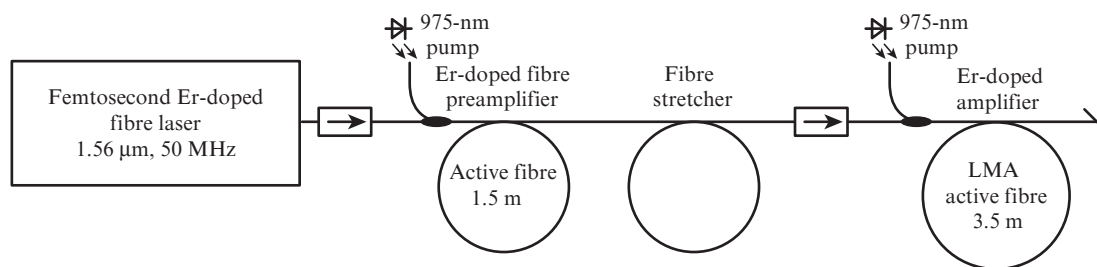


Figure 9. All-fibre configuration with no external compressor.

Figure 10 shows spectra of pulses at the erbium-doped LMA fibre output and the FROG-retrieved temporal intensity profile. The pulse duration is 100 fs and the peak power is estimated at 12 nJ. Note that, in this experiment, a peak power of 100 kW was reached, which was close to the record high value for femtosecond systems with no external compressor [5]. It should be emphasised that, in this case, the peak power was estimated with allowance for the actual pulse

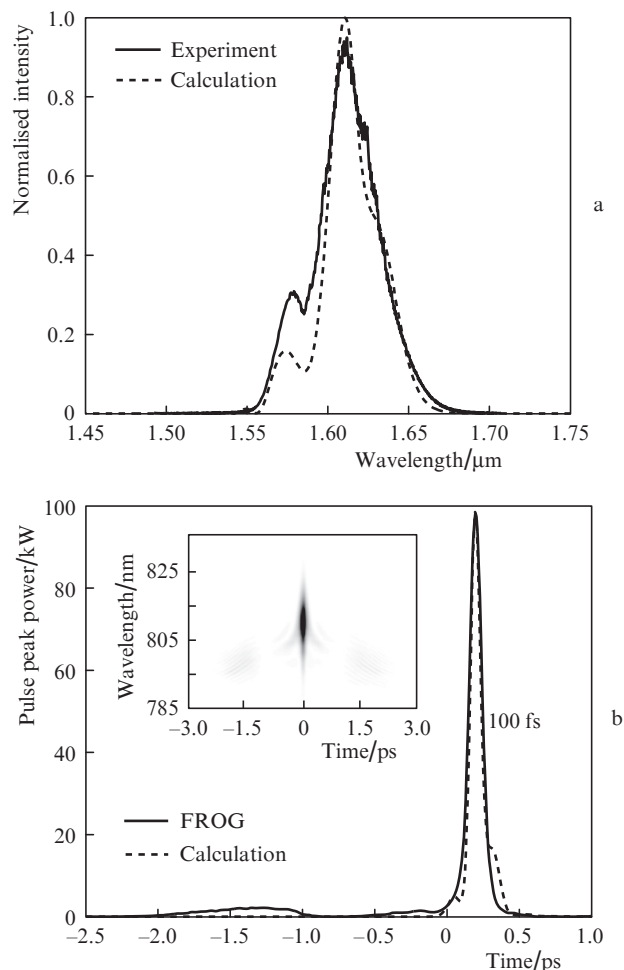


Figure 10. (a) Optical spectra of the signal at the output of an all-fibre configuration with no external compressor: measured with a spectrometer (solid line) and assessed by numerical simulation using Eqn (1) (dashed line); (b) pulse intensity profile retrieved from the measured FROG trace in the inset (solid line) and obtained by numerical simulation (dashed line).

shape (rather than by merely dividing the energy by duration, like in CPA mode).

Further increasing the pump power brought the system away from single-pulse operation and the signal broke up into two or more pulses as a result of the combined effect of self-phase modulation, anomalous dispersion in the amplifier and SRS [20]. Note that, in anomalous dispersion amplifiers, the formation of two synchronised pulses at different wavelengths is possible: upon sequential breakup, the first soliton formed leaves the gain band as a result of the Raman self-frequency shift, and the signal remaining in the gain band is again amplified [21].

The results of mathematical modelling of pulse amplification in erbium-doped LMA fibre are in good quantitative agreement with experimental data (Fig. 10). The spectral and temporal evolution of pulses in erbium-doped active fibres was described using a generalised nonlinear Schrödinger equation, which took into account – in addition to Kerr and Raman nonlinearities and dispersion – a homogeneously broadened gain band corresponding to the ${}^4I_{13/2} \rightarrow {}^4I_{15/2}$ laser transition near $1.5 \mu\text{m}$ [20, 22]:

$$\begin{aligned} & \frac{\partial \tilde{A}(z, \omega)}{\partial z} + \frac{i\beta_2 \omega^2}{2} \tilde{A}(z, \omega) + \frac{i\beta_3 \omega^3}{6} \tilde{A}(z, \omega) \\ & - i\gamma \left(1 + \frac{\omega}{\omega_0}\right) \hat{F} \left[A(z, \tau) \int R(\tau - \eta) |A(z, \eta)|^2 d\eta \right] \\ & = G \exp(-\alpha z) \left(\frac{1}{1 + \omega^2 T_2^2} - \frac{i\omega T_2}{1 + \omega^2 T_2^2} \right) \tilde{A}(z, \omega), \end{aligned} \quad (1)$$

where $\tilde{A}(z, \omega) = \hat{F}[A(z, \tau)]$; \hat{F} is the Fourier transformation operator; $A(z, \tau)$ is the complex electric field envelope; z is a coordinate along the fibre; ω is the circular frequency measured from the centre frequency ω_0 ; τ is the time in the accompanying frame; β_2 and β_3 are the second- and third-order dispersion coefficients; γ is the nonlinearity coefficient; $R(\tau)$ is the Raman response function [19]; α is the unsaturated pump absorption coefficient; the constant G is the maximum gain coefficient; and T_2 is a phenomenological polarization relaxation time. Equation (1) does not take into account gain saturation and, in a more general case, modelling should use the Maxwell–Bloch system of equations [20, 22]. At the same time, the saturation energy estimated by us for an erbium-doped LMA fibre is of the order of $100 \mu\text{J}$. In the case of typical pulse energies, near 10 nJ , gain saturation can be neglected. The population inversion at each point of the fibre remains almost unchanged during a pulse, and the Maxwell–Bloch system of equations reduces to Eqn (1) [20]. Numerical modelling was carried out by the SSFM method using fast Fourier transformation [19].

The nonlinear gain calculated for femtosecond pulses at different stretcher lengths is presented in Fig. 11 as a semilog plot of the pulse duration and a plot of peak power against the distance along the length of active fibre. The calculation results suggest that, indeed, there is an optimal stretcher length, L_{optim} . At stretcher lengths shorter than L_{optim} , the maximum compression point lies within the active fibre, and the pulse has time enough to expand at the amplifier output owing to dispersion effects. The pulse energy at the active fibre output is essentially independent of stretcher length, so the peak power is lower than the optimal one. At stretcher lengths above L_{optim} , the pulse does not reach the maximum

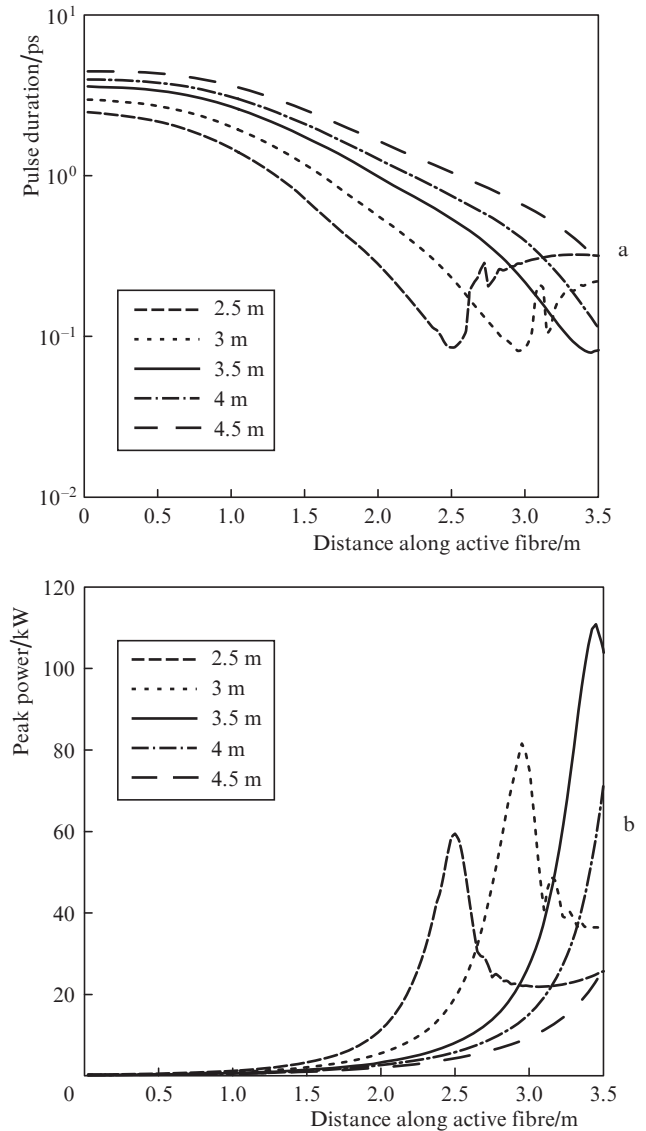


Figure 11. Calculated (a) pulse duration and (b) pulse peak power against the distance along the length of active fibre at different stretcher lengths.

compression point, and the peak power again proves to be lower than the optimal one at the amplifier and input pulse parameters under consideration.

7. Conclusions

We have demonstrated a femtosecond erbium-doped fibre laser system built in the MOPA approach. The final amplifier stage utilises a specially designed erbium-doped LMA fibre. We examined a chirped pulse amplification scheme with the use of a dispersive grating pair compressor and an all-fibre configuration with no external compressor.

In the CPA scheme, we obtained 530-fs pulses at $1.6 \mu\text{m}$ with an energy of 400 nJ . Their peak power is estimated roughly at 750 kW . Such pulses can be effectively converted in nonlinear silica fibre to wavelengths shorter than $1 \mu\text{m}$. We obtained ultra-short 7-nJ pulses with a spectral width of $\sim 100 \text{ nm}$ and a centre wavelength of $0.9 \mu\text{m}$, which can be used as a seed signal in parametric amplifiers of stretched pulses in designing petawatt laser systems. In addition, we

obtained a spectral supercontinuum in the range 0.8–2.2 μm , spanning more than an octave.

In an all-fibre configuration with no external compressor, we obtained 100-fs pulses with an energy of 12 nJ and peak power of ~ 100 kW. Experimental data are supported by mathematic modelling of nonlinear signal amplification in erbium-doped LMA fibre.

Acknowledgements. This research was supported in part by the Presidium of the Russian Academy of Sciences (Extreme Light Fields and Their Applications Programme), the Russian Foundation for Basic Research (Grant Nos 12-08-33101, 13-02-00755 and 14-02-31645) and the RF President's Grants Council (Grant No. MK-5947.2014.2). We are grateful to E.M. Dianov for his continuous interest in and support of this work. E.A. Anashkina acknowledges the support from the Dynasty Nonprofit Foundation.

References

- Richardson D.J., Nilsson J., Clarkson W.A. *J. Opt. Soc. Am. B*, **27**, 63 (2010).
- Fermann M.E., Galvanauskas A., Sucha G., Harter D. *Appl. Phys. B*, **65**, 259 (1997).
- Taverner D., Richardson D.J., Dong L., Caplen J.E., Williams K., Pentyl R.V. *Opt. Lett.*, **22**, 378 (1997).
- Lim E.-L., Alam S., Richardson D.J. *Opt. Express*, **20**, 18803 (2012).
- Jasapara J.C., Andrejco M.J., DeSantolo A., Yablon A.D., Varallyay Z., Nicholson J.W., Fini J.M., DiGiovanni D.J., Headley C., Monberg E., DiMarcello F.V. *IEEE J. Sel. Top. Quantum Electron.*, **15**, 3 (2009).
- Kurkov A.S., Paramonov V.M., Yashkov M.V., Goncharov S.E., Zalevskii I.D. *Kvantovaya Elektron.*, **37**, 343 (2007) [*Quantum Electron.*, **37**, 343 (2007)].
- Austin D.R., de Sterke C.M., Eggleton B.J. *Opt. Express*, **14**, 11997 (2006).
- Roy S., Bhadra S.K., Agrawal G.P. *Phys. Rev. A*, **79**, 023824 (2009).
- Tu H., Lægsgaard J., Zhang R., Tong S., Liu Y., Boppart S.A. *Opt. Express*, **21**, 23188 (2013).
- Andrianov A.V., Anashkina E.A., Muraviov S.V., Kim A.V. *Opt. Lett.*, **35**, 3805 (2010).
- Andrianov A.V., Anashkina E.A., Muravyev S.V., Kim A.V. *Kvantovaya Elektron.*, **43**, 256 (2013) [*Quantum Electron.*, **43**, 256 (2013)].
- Anashkina E.A., Andrianov A.V., Kim A.V. *Kvantovaya Elektron.*, **43**, 263 (2013) [*Quantum Electron.*, **43**, 263 (2013)].
- Khazanov E.A., Sergeev A.M. *Usp. Fiz. Nauk*, **178**, 1006 (2008).
- Lozhkarev V.V., Freidman G.I., Ginzburg V.N., Katin E.V., Khazanov E.A., Kirsanov A.V., Luchinin G.A., Mal'shakov A.N., Martyanov M.A., Palashov O.V., Poteomkin A.K., Sergeev A.M., Shaykin A.A., Yakovlev I.V. *Laser Phys. Lett.*, **4**, 421 (2007).
- Kotov L.V., Likhachev M.E., Bubnov M.M., Medvedkov O.I., Yashkov M.V., Guryanov A.N., Lhermite J., Février S., Cormier E. *Opt. Lett.*, **38**, 2230 (2013).
- Plotskii A.Yu., Kurkov A.S., Yashkov M.Yu., Bubnov M.M., Likhachev M.E., Sysolyatin A.A., Gur'yanov A.N., Dianov E.M. *Kvantovaya Elektron.*, **35**, 559 (2005) [*Quantum Electron.*, **35**, 559 (2005)].
- Likhachev M.E., Bubnov M.M., Zotov K.V., Lipatov D.S., Yashkov M.V., Guryanov A.N. *Opt. Lett.*, **34**, 3355 (2009).
- DeLong K.W., Fittinghoff D.N., Trebino R., Kohler B., Wilson K. *Opt. Lett.*, **19**, 2152 (1994).
- Agrawal G.P. *Nonlinear Fiber Optics* (London: Elsevier, 2013).
- Chi S., Chang C.W., Wen S. *Opt. Commun.*, **106**, 193 (1994).
- Koptev M.Yu., Anashkina E.A., Andrianov A.V., Muravyev S.V., Kim A.V. *Opt. Lett.*, **39**, 2008 (2014).
- Desurvire E. *Erbium-doped Fiber Amplifiers: Principles and Applications* (New York: Wiley-Interscience, 2002).